

Synthetic dimensions with magnetic fields and local interactions in photonic lattices

Tomoki Ozawa and Iacopo Carusotto

INO-CNR BEC Center and Dipartimento di Fisica, Università di Trento, I-38123 Povo, Italy

(Dated: April 14, 2022)

We discuss how one can realize a photonic device that combines synthetic dimensions and synthetic magnetic fields with spatially local interactions. Using an array of ring resonators, the angular coordinate around each resonator spans the synthetic dimension and the synthetic magnetic field arises as the inter-cavity photon hopping is associated to a change of angular momentum. Photon-photon interactions due to the non-linearity of the cavity material are local in the periodic angular coordinate around each ring resonator. Experimentally observable consequences of the synthetic magnetic field and of the local interactions are pointed out.

Quantum simulation of topological models in non-electronic systems has recently received a great interest from a wide community of researchers. Pioneering works made use of ultracold atomic systems, where topological Chern insulator models such as the Harper-Hofstadter model and the Haldane model have been realized in two dimensional optical lattices [1–5]. Almost at the same time, two-dimensional Chern insulator models have also been realized in photonic [6–9] and mechanical systems [10, 11].

Along with these developments, a conceptually novel approach of simulating high-dimensional topological models using “synthetic dimensions” in addition to the physical spatial dimensions has moved its first steps. The idea was first proposed in the context of ultracold atomic gases, where the (discrete) internal spin degrees of freedom of the atoms are regarded as an extra synthetic dimension along which tunneling occurs via suitably designed Raman transitions [12, 13]. While first experimental realizations were restricted to one dimensional lattices [14, 15], this idea holds a prospect of being scaled up to four dimensions using three dimensional optical lattices [16]. In the wake of these pioneering works, an analogous concept of synthetic dimensions have also been proposed for other systems such as atoms in a harmonic potential [17] or photonic systems [18–21].

A common feature of most schemes for synthetic dimensions proposed or realized so far, is that the interaction has a very long or even infinite range along the synthetic direction, which hinders the possibility of simulating standard solid-state physics models based on short-range interactions. As it is still not clear if fractional quantum Hall states or other strongly correlated states can be realized with infinite-range interactions [22, 23], it is of great interest to find schemes to realize synthetic dimensions where interactions are short-ranged.

In this paper, we propose an experimentally realistic strategy to realize a photonic lattice that combines a synthetic dimension and a synthetic magnetic field with local interactions, and therefore has the potential of hosting strongly correlated topologically non-trivial states of matter. We consider an array of ring resonators, but differently from previous proposals [19–21] where the focus

was on the mode index w , the synthetic dimension is here spanned by the geometrical angular coordinate θ around the disk that is conjugate to w . Using a chain of cavities along the x direction, one obtains an effectively two dimensional model in the x - θ plane. A synthetic magnetic field naturally appears if the resonators are designed in a way that hopping along the discrete x direction is accompanied by a change in the angular momentum value w . The photon-photon interactions, induced by a fast optical nonlinearity of the medium, turn out to have the desired local form along both x and θ . The validity of our framework is confirmed by numerical simulations of the cyclotron motion of a wavepacket, and we provide experimentally accessible signatures of the local interactions in the expansion of a suitably initialized wavepacket.

The model Hamiltonian: Our target is to realize a Hamiltonian of the form

$$\mathcal{H} = \sum_x \int_0^{2\pi} d\theta \left[\frac{D}{2} \{i\nabla_\theta b_x^\dagger(\theta)\} \{-i\nabla_\theta b_x(\theta)\} - J \left\{ e^{ic\theta} b_{x+1}^\dagger(\theta) b_x(\theta) + \text{H.c.} \right\} + \frac{U}{2} b_x^\dagger(\theta) b_x^\dagger(\theta) b_x(\theta) b_x(\theta) \right], \quad (1)$$

where $b_x(\theta)$ is an annihilation operator of a photon in a ring cavity at site x with θ being the angular variable around a ring cavity. The site index x is discrete, whereas the angular variable θ is continuous, taking a value $0 \leq \theta < 2\pi$ with periodic boundary conditions $b_x(2\pi) = b_x(0)$. The first term in (1) is the kinetic energy term with an effective mass $1/D$ along the θ direction. The second term describes hoppings between adjacent cavities of (real) amplitude J and a θ -dependent hopping phase equal to $c\theta$ as one hops from sites (x, θ) to $(x+1, \theta)$. The hopping phase represents an effective magnetic field of the strength $B_{\text{eff}} = -c$ in the x - θ plane. Because of the periodicity in the θ direction, the constant c must be an integer. This Hamiltonian describes the motion of a particle on a cylinder with a tight periodic potential along the axial direction, as schematically described in Fig. 1(a). Spatially local photon-photon interactions in the x - θ plane are described by the last term.

In order to see how the Hamiltonian (1) can be physically realized, we Fourier transform the $b_x(\theta)$ operators

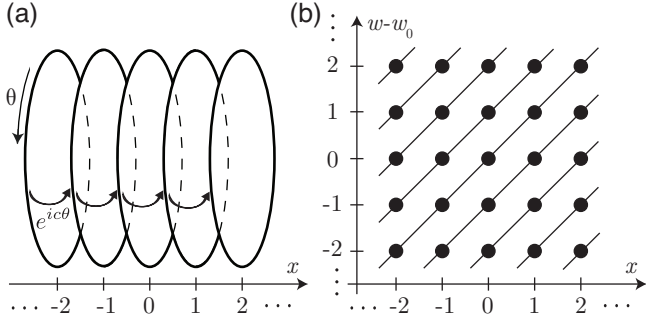


FIG. 1: Schematic illustration of hoppings (a) in the x - θ plane and (b) in x - w plane when $c = 1$.

to the conjugate angular momentum w space:

$$b_{x,w} \equiv \sqrt{\frac{1}{2\pi}} \int_0^{2\pi} d\theta b_x(\theta) e^{-i(w-w_0)\theta}; \quad (2)$$

the reference angular momentum w_0 is introduced here for later convenience. In terms of the transformed $b_{x,w}$ operators, the Hamiltonian (1) is rewritten in the form

$$\begin{aligned} \mathcal{H} = & \sum_{x,w} \frac{D}{2} (w - w_0)^2 b_{x,w}^\dagger b_{x,w} - J \sum_{x,w} \left(b_{x+1,w+c}^\dagger b_{x,w} + \text{H.c.} \right) \\ & + \frac{U}{4\pi} \sum_x \sum_{w_1+w_2=w_3+w_4} b_{x,w_1}^\dagger b_{x,w_2}^\dagger b_{x,w_3} b_{x,w_4}. \quad (3) \end{aligned}$$

The hopping between adjacent cavities, described by the second term, is accompanied by a change of c units of angular momentum w . These hopping processes in the x - w plane are schematically described in Fig. 1(b). The last term represents the inter-photon interaction which conserves the total angular momentum.

Physical implementation: Among its many possible realization, the Hamiltonian (3) can be engineered using an array of coupled ring resonators with different sizes and shapes. In particular, we propose to design cavities in a way that their mode frequencies depend on x and w as

$$\Omega_{x,w} = \Omega_0 + \Omega_{\text{FSR}}(w - w_0 - xc) + D(w - w_0)^2/2. \quad (4)$$

where Ω_0 is the frequency of a reference mode $w_0 \gg 1$ in the central $x = 0$ cavity and we restrict our attention to $w > 0$ modes. The free spectral range of the cavities is Ω_{FSR} and the quadratic dispersion term D accounts for deviations from perfect mode equispacing. In particular, the modes of neighboring cavities are assumed to be shifted by $-c\Omega_{\text{FSR}}$, so that $\Omega_{x,w} \approx \Omega_{x+1,w+c}$.

Possible experimental setups for realizing our proposal are an array of silicon micro-ring resonators [8] or an array of exciton-polariton micropillars [24]. In both cases, the condition (4) can be obtained by careful fabrication

of cavities adjusting available parameters such as the radius and the shape of the section of cavities [25].

If the hopping is much smaller than the free spectral range $J \ll \Omega_{\text{FSR}}$, since $\Omega_{x,w} \approx \Omega_{x+1,w+c}$, the only effective tunneling processes are the ones associated by an angular momentum change by c . Assuming that the relevant amplitude does not significantly depend on x nor on w , the non-interacting tight-binding Hamiltonian is

$$\begin{aligned} \tilde{\mathcal{H}}_0 = & \sum_{x,w} \Omega_{x,w} a_{x,w}^\dagger a_{x,w} - J \sum_{x,w} \left(a_{x+1,w+c}^\dagger a_{x,w} + \text{H.c.} \right), \quad (5) \end{aligned}$$

where $a_{x,w}$ is the annihilation operators for a photon with the angular momentum w at site x . Moving to a rotating frame by $b_{x,w} \equiv a_{x,w} \exp\{i[\Omega_0 + \Omega_{\text{FSR}}(w - w_0 - xc)]t\}$, one immediately recovers the non-interacting part of the desired Hamiltonian (3). The origin of the synthetic magnetic field can be understood by noting that in terms of the rescaled $\tilde{w} = w - w_0 - xc$, which does not change during tunneling, the mode frequency (4) recovers the one of a free particle in a magnetic field with Landau-gauge with a boost in the synthetic direction, $\Omega_{x,\tilde{w}} = \Omega_0 + \Omega_{\text{FSR}}\tilde{w} + \frac{D}{2}(\tilde{w} + xc)^2$, where \tilde{w} is analogous to momentum in the synthetic dimension.

The photons in a cavity can interact via the nonlinearity of the underlying medium. The electric field $\mathbf{E}(\mathbf{r}, t)$ in a cavity placed at the origin ($x = 0$) can be written as

$$\mathbf{E}(\mathbf{r}, t) = \sum_w \left(\mathcal{E}_w(\mathbf{r}) a_{0,w} + \mathcal{E}_w^*(\mathbf{r}) a_{0,w}^\dagger \right), \quad (6)$$

where, assuming a circular form for the cavity and restricting to radially polarized modes, the electric index profile $\mathcal{E}^w(\mathbf{r})$ of the mode w in the cylindrical coordinates (r, ϕ, z) has the form $\mathcal{E}^w(\mathbf{r}) = R_w(r) Z_w(z) e^{iw\phi} \hat{e}_r$ where \hat{e}_r is the unit vector in the radial direction. Assuming that the $\chi^{(3)}$ nonlinearity is local in space and sufficiently fast in time, the photon-photon interactions within the $x = 0$ cavity are described by the Hamiltonian

$$\mathcal{H}_{\text{int},x=0} = \tilde{U} \int d^3r |\mathbf{E}(\mathbf{r}, t)|^4. \quad (7)$$

Inserting (6) into (7), one notices that only angular momentum conserving terms survive after the integration over \mathbf{r} . Under the rotating wave approximation, we ignore terms involving unequal numbers of creation and annihilation operators. Grouping all numerical factors into the coefficient U , one obtains the following interaction Hamiltonian in the rotating basis

$$\mathcal{H}_{\text{int},x=0} = \frac{U}{4\pi} \sum_{w_1+w_2=w_3+w_4} b_{0,w_1}^\dagger b_{0,w_2}^\dagger b_{0,w_3} b_{0,w_4}, \quad (8)$$

which is straightforwardly extended to the many-cavity case described in our target Hamiltonian (3).

The assumed condition for a local interaction in θ requires that the nonlinearity be sufficiently fast on the time scale of Ω_{FSR} . If the interaction is slow, each term in (8) is multiplied by a coefficient which is a function of $\Omega_{\text{FSR}}(w_1 - w_4)$ that decays on the scale of the inverse response time of the medium. This condition can be physically understood by noting that a photon wavepacket quickly rotates around the ring cavity at an angular speed Ω_{FSR} . Transformation to the $b_{x,w}$ operators corresponds to moving to a reference frame that rotates at this speed.

Single-particle physics: After having introduced the general model and proposed its experimental implementation, we now turn our attention to the single-particle (non-interacting) physics predicted by the model Hamiltonian (1). This Hamiltonian describes a quantum particle subject to a magnetic field and moving in a hybrid geometry with one discrete and one continuous dimension. A free charged particle in a magnetic field with two continuous dimensions is a text-book problem leading to highly degenerate Landau levels [26]. On the other hand, the same problem in two discrete dimensions is known as the Harper-Hofstadter model and leads to the energy spectrum known as the Hofstadter butterfly [27]. The configuration considered here lies in between the two cases of Landau levels and of the Hofstadter butterfly.

When the system is periodic in the x direction, the Hamiltonian (1) is translationally invariant in the x direction, so one can take advantage of the conserved momentum k_x and express $b_x(\theta) = \frac{1}{\sqrt{N_x}} \sum_{k_x} e^{ik_x x} b(k_x, \theta)$, where N_x is the number of cavities along x . The problem is then reduced to the one dimensional Hamiltonian

$$\mathcal{H}_0 = \sum_{k_x} \int_0^{2\pi} d\theta \left[\frac{D}{2} (i\nabla_\theta b^\dagger(k_x, \theta) (-i\nabla_\theta b_x(k_x, \theta)) - 2J \cos(c\theta - k_x) b^\dagger(k_x, \theta) b(k_x, \theta)) \right] \quad (9)$$

describing mass of $1/D$ particles moving in a cosine-shaped potential with periodic boundary conditions $\theta + 2\pi = \theta$. As the k_x dependence in the potential $\cos(c\theta - k_x)$ can be absorbed into the shift of the origin of the periodic coordinate θ , the one-particle spectrum does not depend on k_x . This implies that each state is N_x -fold degenerate, which is reminiscent of Landau levels.

In the limit of large D , the harmonic trapping in w direction dominates over the hopping along x , and the spectrum becomes $n^2 D/2$, where n is an integer. In the opposite $D \ll J$ limit, when $c \neq 0$, the cosine potential $-2J \cos(c\theta)$ is large compared to the kinetic energy, therefore the low-lying energy levels of the system can be obtained with a quadratic approximation of the cosine potential around each of its $|c|$ minima. As in a harmonic oscillator, the energy levels are then approximately equispaced $E_n = -2J + \sqrt{2D/J} (n + 1/2) cJ$, where $n \geq 0$ is a non-negative integer and, for a given value of k_x , each of them is approximately $|c|$ -fold degenerate. The splitting due to tunneling between minima of the cosine potential

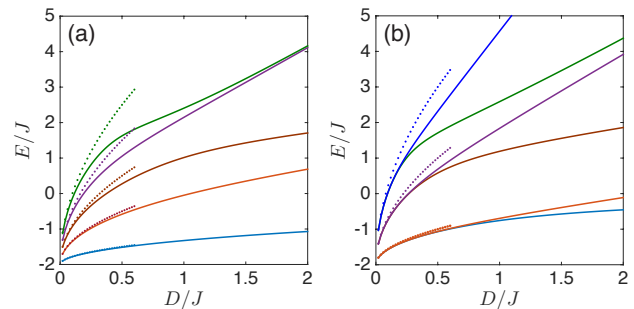


FIG. 2: Energy levels as a function of D/J for (a) $c = 1$ and (b) $c = 2$. The solid lines show the numerically obtained first (a) five and (b) six energy eigenvalues, and the dotted lines are the analytical approximations for $D/J \ll 1$.

is exponentially small in the $D \rightarrow 0$ limit. In Fig. 2, we plot the first several single particle energy levels as one varies D for $c = 1$ and 2 : a very good agreement is found at small D between the asymptotic analytical expression (dotted lines) and the full spectrum (solid lines).

Because of its intrinsic periodicity in θ , our system does not have any edge in θ . Open boundary conditions can be chosen along x , which lead to chiral edge states, whose properties are similar to the Landau level problem; more details are discussed in the Supplemental Material [28]. In what follows, we focus our attention on experimentally observable magnetic and interaction effects in the bulk.

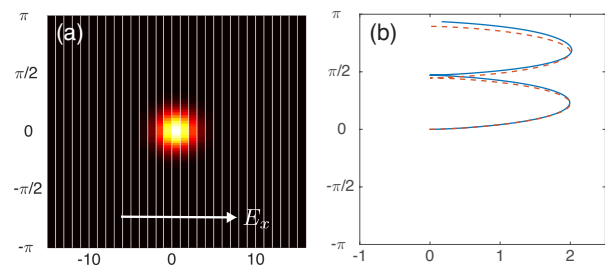


FIG. 3: Cyclotron motion of a wave packet for $N_x = 31$, $D = 0.1J$, $c = 1$, $UN = 20J$, and $E_x = 0.1J$, where N is the total number of photons. In both (a) and (b), the horizontal axis is x and the vertical axis is θ . The initial condition of the wave packet is plotted in (a). In (b), the center-of-mass motion of the wavepacket from $t = 0$ to $4\pi/\omega_c$ is plotted. The solid line is from the numerical simulation of the dynamics of the wavepacket, and the dashed line is the analytical prediction from Eq. (11).

Cyclotron orbits: As a first example, we investigate the semiclassical cyclotron orbits of a Gaussian wave packet in the x - θ plane. Such a wave packet can be created by a Gaussian pulse in the x direction which overlaps with many w modes of each cavity. This can be obtained if each cavity is locally coupled to the waveguide where

the pulse is launched, so that the temporal shape of a short pulse of duration $\tau_P \ll \Omega_{\text{FSR}}^{-1}$ gets transferred to the initial profile of the wavepacket along θ .

In order to observe non-trivial orbits, we assume there is a constant force applied to x direction, which can be implemented via an additional small constant frequency gradient of cavities along x direction. Provided the initial wavepacket is large enough to only explore the harmonic region of the spectrum at small D , the center-of-mass of the wave packet follows the semiclassical cyclotron orbit determined by the classical equations of motion:

$$\begin{aligned} m_x dv_x(t)/dt &= E_x + B_{\text{eff}} v_\theta(t), \\ m_\theta dv_\theta(t)/dt &= -B_{\text{eff}} v_x(t), \end{aligned} \quad (10)$$

where $m_x = 1/2J$ and $m_\theta = 1/D$ are the effective masses in x and θ directions and $v_x(t)$ and $v_\theta(t)$ are the velocities of the center-of-mass at time t in x and θ directions, respectively. The constant force E_x is applied in x direction. Solving the equations under the initial conditions $x = v_x = v_\theta = 0$ at $t = 0$, the wavepacket trajectory in time follows the curve:

$$\begin{aligned} \langle x(t) \rangle &= (E_x/B_{\text{eff}}^2) 2m_\theta \sin^2(\omega_c t/2), \\ \langle \theta(t) \rangle &= (E_x/B_{\text{eff}}^2) \sqrt{m_x m_\theta} \sin(\omega_c t) - (E_x/B_{\text{eff}}) t, \end{aligned} \quad (11)$$

where $\omega_c \equiv B_{\text{eff}}/\sqrt{m_x m_\theta}$ is the cyclotron frequency.

In Fig. 3, we compare the analytical semiclassical prediction (11) for the center-of-mass motion of a wavepacket obtained with a full numerical solution of the Hamiltonian (1) including interactions at the mean-field level. The agreement is good and, as expected, improves even further if smaller values of D are used.

Expansion dynamics: As a last point, we now present a scheme to experimentally assess the local nature of the photon-photon interactions. We now assume there is no force ($E_x = 0$), and we treat the interactions at the mean-field level. In absence of an effective magnetic field (i.e. $c = 0$), a circularly symmetric Gaussian wavepacket in the x - θ plane maintains its circular symmetry during its expansion provided scaled axes are used so that the effective masses in the two directions are the same. (This can be achieved by introducing a scaled variable $y \equiv \theta\sqrt{2J/D}$ and preparing a symmetric wave packet in x - y plane.). In the presence of a magnetic field ($c \neq 0$), the wavepacket expansion is symmetric only when one has a rotationally symmetric gauge. Our Hamiltonian (1) is written in the Landau gauge where non-trivial hopping phases are present only along one direction. In order to observe a symmetric expansion, one needs to prepare a Gaussian wave packet with an appropriate phase, which corresponds to a gauge transformation from the Landau gauge to the symmetric gauge [29, 30].

In Fig. 4, we plot how such a suitably designed wave packet expands after half the period of the cyclotron motion in different cases. Panel (a) shows the initial condition of the wave packet. Panel (b) shows the expanded

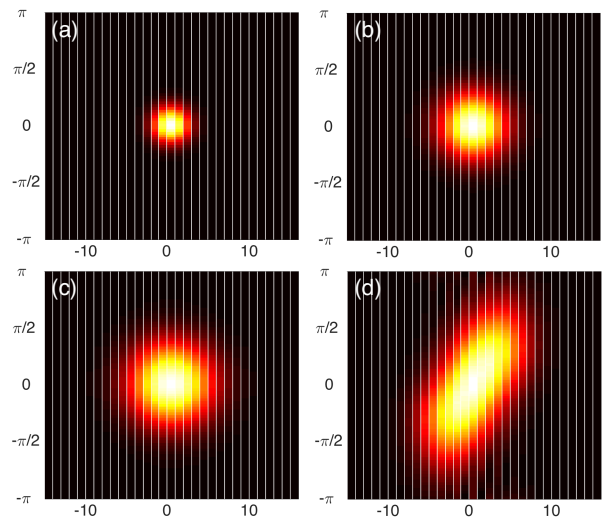


FIG. 4: Free expansion of a Gaussian wave packet for $c = 1$ and $D = 0.1J$ after the expansion time of π/ω_c . (a) The initial wave packet. (b) The expansion in the absence of the interaction. (c) The expansion in the presence of the contact interaction with $UN = 20J$. (d) The expansion in the presence of the infinite-range interaction with $U_{\text{inf}}N = 5J$. The horizontal axes are x , and the vertical axes are θ .

wavepacket in the absence of interactions, when the ballistic expansion is due to diffraction. Panel (c) shows the expanded wavepacket for local interactions: interactions speed up the expansion, but the wavepacket always maintains its initial symmetric shape as expected.

For comparison, panel (d) shows the expansion for the infinite-ranged nonlocal interactions along θ of the form: $\mathcal{H}_{\text{inf}} = \frac{U_{\text{inf}}}{2} \sum_x \left(\int_0^{2\pi} d\theta b_x^\dagger(\theta) b_x(\theta) \right)^2$ that one would obtain, e.g., in the case of a temporally slow non-linearity. In this case, the expansion along the θ direction does not initially feel the effect of the infinite-range interaction in the θ direction and is thus concentrated in the x direction. At later times, the elongated wave packet then rotates due to the synthetic Lorentz force induced by the synthetic magnetic field, which gives rise to the non-symmetric final shape. Comparison of panels (c) and (d) then shows a clear and experimentally observable signature of the local vs. nonlocal of interactions.

Outlook: In this Letter we have shown how synthetic dimensions with magnetic fields and local interactions can be created using an array of nonlinear optical cavities. As our scheme can be straightforwardly extended up to three spatial dimensions, a most exciting perspective is to study the physics of interacting Bose gases in four dimensions. Given the local nature of interactions in our proposed set-up, this opens unprecedented possibilities to experimentally study the intriguing new features of fractional quantum Hall physics and topological effects in high dimensions [31, 32].

We are grateful to Hannah Price for stimulating discussions, and we also thank valuable discussions with Nathan Goldman and Thomas Scaffidi. We thank Fernando Ramiro Manzano and Zeno Gaburro for useful exchanges on silicon micro-ring resonators, and Albert Adiyatullin and Claud eric Ouellet-Plamondon for helpful discussions on their exciton-polariton micropillars. This work was funded by ERC through the QGBE grant, by the EU-FET Proactive grant AQuS, Project No. 640800, and by the Provincia Autonoma di Trento, partially through the project ‘‘On silicon chip quantum optics for quantum computing and secure communications – SiQuero’’.

-
- [1] M. Aidelsburger, M. Atala, M. Lohse, J. T. Barreiro, B. Paredes, and I. Bloch, *Realization of the Hofstadter Hamiltonian with Ultracold Atoms in Optical Lattices*, Phys. Rev. Lett. **111**, 185301 (2013).
- [2] H. Miyake, G. A. Siviloglou, C. J. Kennedy, W. C. Burton, and W. Ketterle, *Realizing the Harper Hamiltonian with Laser-Assisted Tunneling in Optical Lattices*, Phys. Rev. Lett. **111**, 185302 (2013).
- [3] M. Aidelsburger, M. Lohse, C. Schweizer, M. Atala, J. T. Barreiro, S. Nascimbene, N. R. Cooper, I. Bloch, and N. Goldman, *Measuring the Chern number of Hofstadter bands with ultracold bosonic atoms*, Nature Physics **11**, 162 (2015).
- [4] C. J. Kennedy, W. C. Burton, W. C. Chung, and W. Ketterle, *Observation of Bose-Einstein condensation in a strong synthetic magnetic field*, Nature Physics **11**, 859 (2015).
- [5] G. Jotzu, M. Messer, R. Desbuquois, M. Lebrat, T. Uehlinger, D. Greif, and T. Esslinger, *Experimental realization of the topological Haldane model with ultracold fermions*, Nature **515**, 237 (2015).
- [6] M. C. Rechtsman, J. M. Zeuner, Y. Plotnik, Y. Lumer, D. Podolsky, F. Dreisow, S. Nolte, M. Segev, and A. Szameit, *Photonic Floquet topological insulators*, Nature **496**, 196 (2013).
- [7] M. Hafezi, E. A. Demler, M. D. Lukin, and J. M. Taylor, *Robust optical delay lines with topological protection*, Nature Physics **7**, 907 (2011).
- [8] M. Hafezi, S. Mittal, J. Fan, A. Migdall, and J. M. Taylor, *Imaging topological edge states in silicon photonics*, Nature Photonics **7**, 1001 (2013).
- [9] J. Ningyuan, C. Owens, A. Sommer, D. Schuster, and J. Simon, *Time- and Site-Resolved Dynamics in a Topological Circuit*, Phys. Rev. X **5**, 021031 (2015).
- [10] R. S usstrunk and S. D. Huber, *Observation of phononic helical edge states in a mechanical topological insulator*, Science **349**, 47 (2015).
- [11] L. M. Nash, D. Kleckner, A. Read, V. Vitelli, A. M. Turner, and W. T. M. Irvine, *Topological mechanics of gyroscopic metamaterials*, Proceedings of the National Academy of Sciences **112**, 14495 (2015).
- [12] O. Boada, A. Celi, J. I. Latorre, and M. Lewenstein, *Quantum Simulation of an Extra Dimension*, Phys. Rev. Lett. **108**, 133001 (2012).
- [13] A. Celi, P. Massignan, J. Ruseckas, N. Goldman, I. B. Spielman, G. Juzelinas, and M. Lewenstein, *Synthetic Gauge Fields in Synthetic Dimensions*, Phys. Rev. Lett. **112**, 043001 (2014).
- [14] M. Mancini, G. Pagano, G. Cappellini, L. Livi, M. Rider, J. Catani, C. Sias, P. Zoller, M. Inguscio, M. Dalmonte, and L. Fallani, *Observation of chiral edge states with neutral fermions in synthetic Hall ribbons*, Science **349**, 1510 (2015).
- [15] B. K. Stuhl, H. I. Lu, L. M. Aycock, D. Genkina, and I. B. Spielman, *Visualizing edge states with an atomic Bose gas in the quantum Hall regime*, Science **349**, 1514 (2015).
- [16] H. M. Price, O. Zilberberg, T. Ozawa, I. Carusotto, and N. Goldman, *Four-Dimensional Quantum Hall Effect with Ultracold Atoms*, Phys. Rev. Lett. **115**, 195303 (2015).
- [17] H. Price, T. Ozawa, and N. Goldman, *Synthetic Dimensions for Cold Atoms from Shaking a Harmonic Trap*, arXiv:1605.09310.
- [18] M. Schmidt, S. Kessler, V. Peano, O. Painter, and F. Marquardt, *Optomechanical creation of magnetic fields for photons on a lattice*, Optica **2**, 635 (2015).
- [19] X.-W. Luo, J.-S. Xu, G.-C. Guo, X. Zhou, C.-F. Li, and Z.-W. Zhou, *Quantum simulation of 2D topological physics in a 1D array of optical cavities*, Nature Communications **6**, 1 (2015).
- [20] T. Ozawa, H. M. Price, N. Goldman, O. Zilberberg, and I. Carusotto, *Synthetic dimensions in integrated photonics: From optical isolation to four-dimensional quantum Hall physics* Phys. Rev. A **93**, 043827 (2016).
- [21] L. Yuan, Y. Shi, and S. Fan, *Photonic gauge potential in a system with a synthetic frequency dimension*, Optics Letters **41**, 741 (2016).
- [22] S. Barbarino, L. Taddia, D. Rossini, L. Mazza, and R. Fazio, *Magnetic crystals and helical liquids in alkaline-earth fermionic gases*, Nature Commun. **6**, 8134 (2015).
- [23] M. Ła cki, H. Pichler, A. Sterdyniak, A. Lyras, V. E. Lembessis, O. Al-Dossary, J. C. Budich, and P. Zoller, *Quantum Hall physics with cold atoms in cylindrical optical lattices*, Phys. Rev. A **93**, 013851 (2016).
- [24] C. Ouellet-Plamondon, G. Sallen, F. Morier-Genoud, D. Y. Oberli, M. T. Portella-Oberli, and B. Deveaud, *Spatial multistability induced by cross interactions of confined polariton modes*, Phys. Rev. B **93**, 085313 (2016).
- [25] F. Ramiro Manzano, private communications.
- [26] L. D. Landau and E. M. Lifshitz, *Quantum Mechanics* (Butterworth-Heinemann, Oxford, 1977).
- [27] D. Hofstadter, *Energy levels and wave functions of Bloch electrons in rational and irrational magnetic fields*, Phys. Rev. B **14**, 2239 (1976).
- [28] See Supplemental Material.
- [29] H. Y. Kim and J. H. Weiner, *Gaussian-Wave-Packet Dynamics in Uniform Magnetic and Quadratic Potential Fields*, Phys. Rev. B **7**, 1353 (1973).
- [30] H. Tsuru, *Wave Packet Motion in Magnetic Field*, J. Phys. Soc. Japan **61**, 2246 (1992).
- [31] S.-C. Zhang, J. Hu, *A Four-Dimensional Generalization of the Quantum Hall Effect*, Science **294** 823 (2001).
- [32] E. Dennis, A. Kitaev, A. Landahl, and J. Preskill, *Topological quantum memory*, J. Math. Phys. **43**, 4452 (2002).

Supplemental Material for “Synthetic dimensions with magnetic fields and local interactions in photonic lattices”

Tomoki Ozawa and Iacopo Carusotto

INO-CNR BEC Center and Dipartimento di Fisica, Università di Trento, I-38123 Povo, Italy

(Dated: April 14, 2022)

Appendix A: Edge properties of the model

In this Supplemental Material, we provide details on the edge properties of the Hamiltonian (1) of the main text in the absence of interactions. It is convenient to work in the Fourier transformed representation, Eq. (3) in the main text, which reads

$$\mathcal{H} = \sum_{x,w} \frac{D}{2} (w - w_0)^2 b_{x,w}^\dagger b_{x,w} - J \sum_{x,w} \left(b_{x+1,w+c}^\dagger b_{x,w} + \text{H.c.} \right) \quad (\text{A.1})$$

The Hamiltonian can be made diagonal in w by introducing a shifted operator

$$b_{x,w} = \tilde{b}_{x,w-cx}. \quad (\text{A.2})$$

In terms of the shifted operator, the Hamiltonian becomes

$$\begin{aligned} \mathcal{H} &= \sum_{x,k_\theta} \frac{D}{2} (w - w_0)^2 \tilde{b}_{x,w-cx}^\dagger \tilde{b}_{x,w-cx} \\ &\quad - J \left\{ \tilde{b}_{x+1,w-cx}^\dagger \tilde{b}_{x,w-cx} + \text{H.c.} \right\} \\ &= \sum_{x,w} \frac{D}{2} (w - w_0 + cx)^2 \tilde{b}_{x,w}^\dagger \tilde{b}_{x,w} \\ &\quad - J \left\{ \tilde{b}_{x+1,w}^\dagger \tilde{b}_{x,w} + \text{H.c.} \right\}, \end{aligned} \quad (\text{A.3})$$

which is diagonal in w . By diagonalizing this Hamiltonian for a given value of w with an open boundary condition in x direction, we obtain the energy spectrum of the system in the presence of edges in x direction. One can observe that the first term acts as a harmonic trapping potential in x direction, centered at $-(w - w_0)/c$; this structure is very similar to the case of an ordinary two dimensional Landau level problem in the Landau gauge. As in the Landau level problem, the effect of the finite size of the system is felt when the center of the trapping potential $-(w - w_0)/c$ reaches the edge.

In Fig. 1, we plot the spectrum as a function of $w - w_0$, calculated for a system with $N_x = 41$ sites in x direction

with $c = 1$, and we chose $-20 \leq x \leq 20$. The spectrum is reminiscent of the Landau level problem. There are flat levels for small values of $|w - w_0|$, which are bulk degenerate levels of the system. In the region where $|w - w_0|$ is large and of order $cN_x/2$, the harmonic oscillator center in (A.3) reaches the edge of the systems, and the energy levels are not flat anymore. We find that the wavefunctions satisfying $w - w_0 \gtrsim cN_x/2$ are localized at the right edge of the array, whereas the wavefunctions satisfying $w - w_0 \lesssim -cN_x/2$ are localized at the left edge. The states with $w - w_0 \gtrsim cN_x/2$ localized at the right edge have a positive group velocity, thereby forming edge states which move only in the positive θ direction. On the other hand, the states with $w - w_0 \lesssim -cN_x/2$ localized at the left edge have a negative group velocity, forming edge states which move only in the negative θ direction. This unidirectionality of states localized at the edge indicates that we have chiral edge states, which are characteristic of two dimensional topological models with time-reversal symmetry breaking.

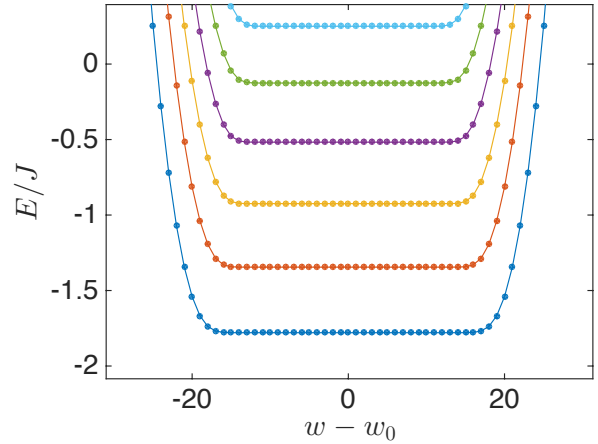


FIG. 1: The energy spectrum as a function of $w - w_0$ under the open boundary condition for $N_x = 41$. We chose $D = 0.1J$ and $c = 1$. Since $w - w_0$ can take only integer values, the lines connecting the dots are just a guide to the eye.